



Microwave Orbital Angular Momentum Beam Generation Based on Circularly Polarized Metasurface Antenna Array

Jianchun Xu,¹ Yanan Hao,¹ Ke Bi,^{1*} Ru Zhang,¹ Shanguo Huang^{1*} and Ji Zhou^{2*}

A V-shaped metasurface structure is applied in the design of circularly polarized antenna for excellent polarization performance. By means of structural parameter optimization, a 0.34 dB axial ratio is obtained. This proposed antenna has a compact dimension of $0.272\lambda_0 \times 0.272\lambda_0 \times 0.02\lambda_0$, which is beneficial for the practical applications. Several proposed metasurface antennas are fabricated and measured to verify the rationality of design. The simulated and measured results of the OAM beams well demonstrate the capability of this circularly polarized metasurface antenna array in generating OAM beam.

Keywords: Metasurface; Orbital angular momentum; Antenna array

Received 29 January 2019, **Accepted** 11 February 2019

DOI: 10.30919/es8d748

1. Introduction

Nowadays, wireless system manufacturers desire compact, easily fed, circularly polarized (CP) antennas.¹ Compared to the linearly polarized (LP) antenna, CP antenna is more attractive due to the lower signal loss caused by mismatch between the polarization of transmitting and receiving antennas.^{2,4} Therefore, CP antenna is more suitable for portable devices, mobile wireless, satellite communication, etc.⁵⁻⁷ Generally, CP waves are excited by two orthogonal modes with 90° phase difference. The slot structures,⁸ truncated corners patch⁹ and feed-line network¹⁰ are usually used to stimulate these modes for the design of CP antenna. However, these methods do not perform well in terms of ratio axial (AR), gain and volume.

Metasurface, an artificially structured material, has become a research frontier and received a fast development because of their remarkable features that is not readily available in nature.¹¹⁻¹⁴ Compared to traditional three-dimensional structures, metasurfaces possess miniature and ultrathin characteristics.¹⁵ Therefore, they are easier to be fabricated and integrated in devices or systems.¹⁶⁻¹⁹ Moreover, metasurfaces are much more flexible to accurately tailor the amplitude, phase and polarization of electromagnetic wave.²⁰⁻²² Thus, it is highly suitable for the design of CP antenna. More importantly, utilization of metasurface structure in CP antenna design can improve the electromagnetic properties without increasing the antenna size.

Recently, orbital angular momentum (OAM) has attracted extensive attention due to its exotic electromagnetic properties in

improving channel capacity.^{23,24} Although there are some debates on whether the additional capacity of multiple-in-multiple-out (MIMO) systems can be obtained by using the OAM radio communication,²⁵ the potential applications in other fields, such as electromagnetic vortex imaging, quantum state manipulation and radar detection, still keep the researchers' enthusiasm in studying OAM.^{26,27}

In this work, we adopt V-shaped gap as the metasurface unit cell to design the compact CP antenna. The structure parameters of the antenna were studied to verify the merits of adopting metasurface structure in CP antenna. After optimization, all the parameters were determined and the prototype antennas were fabricated and measured. As shown in Fig. 1, an antenna array constituted by six proposed circularly polarized antennas was designed to generate the radio OAM beams. The phase difference of adjacent antennas is adjusted by rotation of the antennas. OAM beams can be generated by the interference between the electromagnetic waves transmitted by the antennas. To verify the capability of the metasurface antenna array in generating OAM beams, a measured system was designed. All the simulated and measured results demonstrate that a well-structured circularly polarized

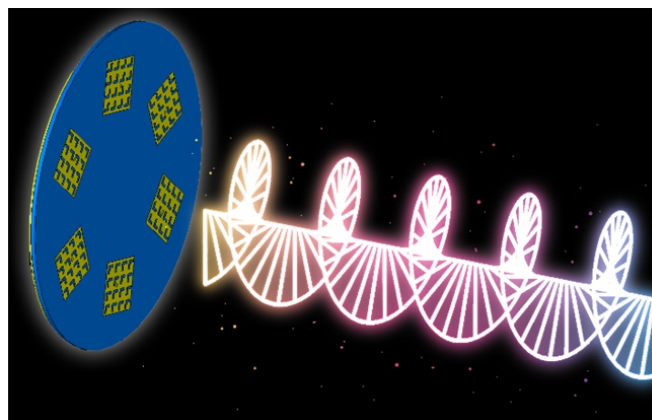


Fig. 1 Prototype of the OAM beam generation.

¹State Key Laboratory of Information Photonics and Optical Communications, School of Science, Beijing University of Posts and Telecommunications, Beijing 100876, China

²State Key Laboratory of New Ceramics and Fine Processing, School of Materials Science and Engineering, Tsinghua University, Beijing 100084, China

*E-mail: bike@bupt.edu.cn; shghuang@bupt.edu.cn; zhouji@tsinghua.edu.cn

metasurface antenna was acquired for generating OAM beams, which can improve the OAM beams' practical applications in wireless communications, rotational speed measurement, radar and so on.

2. Design of the circularly polarized metasurface antenna

The V-shaped metal robs can support “symmetric” and “antisymmetric”

modes.²⁸ These two modes are adopted to meet the need for designing circularly polarized antenna. Besides, the orthogonality, 90 degree phase difference and equal magnitude are easily satisfied by changing the length, angular, width and feed point position. It means that the circular polarization is easy to be realized. Thus, the V-shaped structure is used as unit cell of the metasurface in the radiation patch. Considering the size of antenna and machining accuracy, the 4×4 unit cells are suitable.

The geometry of the circularly polarized metasurface antenna is

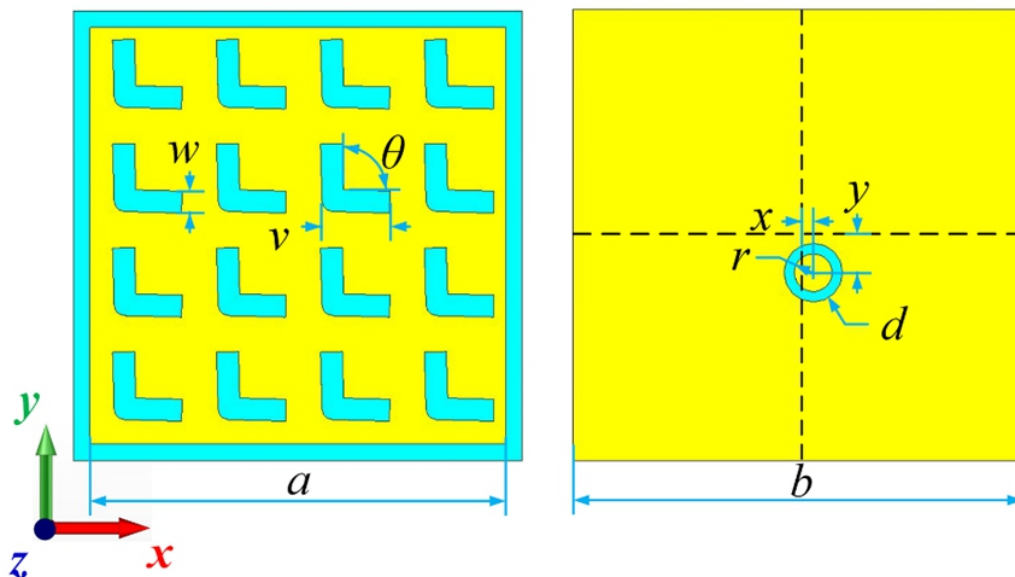


Fig. 2 Schematic diagram of the circularly polarized metasurface antenna.

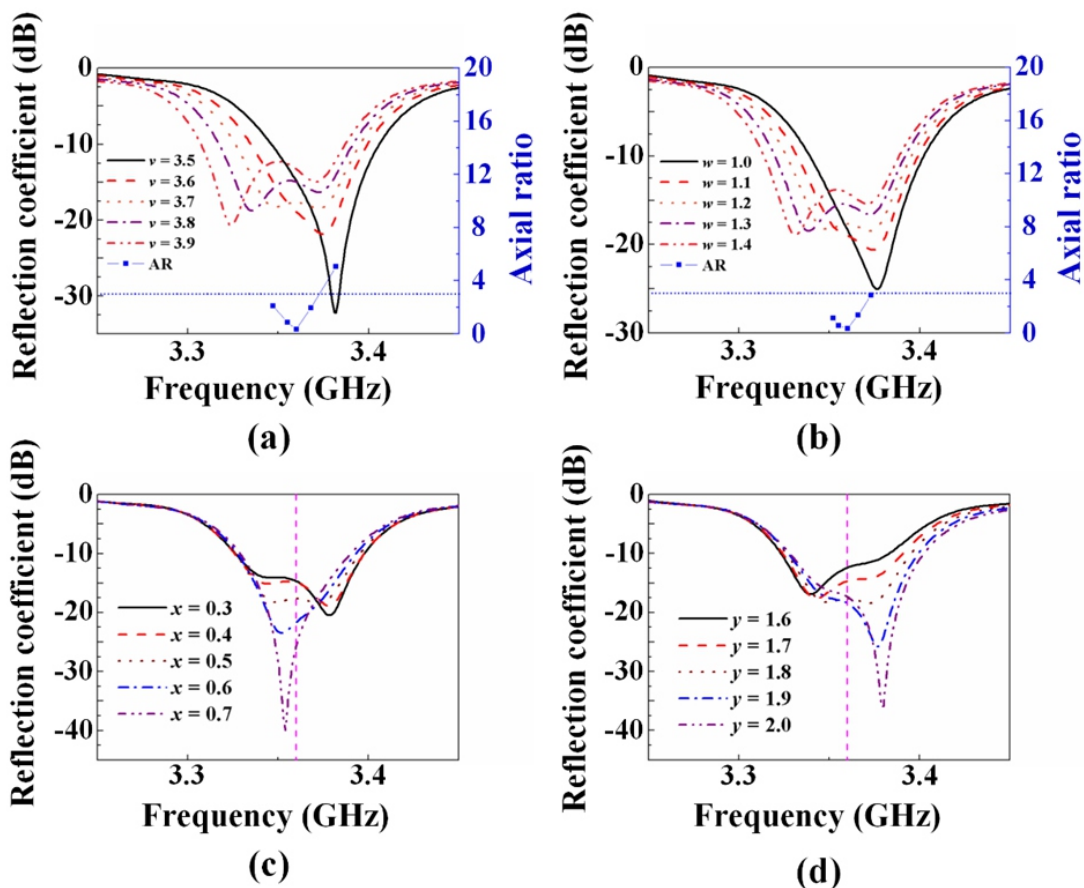


Fig. 3 Simulated reflection coefficients and their axial ratio (AR) of the proposed antenna with a series of (a) v , (b) w , (c) x and (d) y .

plotted in Fig. 2. The proposed antenna is composed of radiation patch, dielectric substrate and ground plane. Here, the coaxial feeding technique is adopted. The circular loop shown in Fig. 2 depicts its position and dimensions. In order to provide enough space for the feed point, the angle θ is set as about 90 degree. All the V-shaped unit cells are uniformly distributed on the radiation patch. Thus, the periodicity of the unit cell is $a/4$. This metasurface structure is loaded on a commercial printed circuit board, F4B, with a relative permittivity of 3.5. The resonance frequency of antenna is mainly affected by size of the three layers.

To find out the optimum parameters, numerical predictions of the reflection coefficients for the proposed antenna were simulated by using the commercial time-domain package CST Microwave Studio. Among them, the width w and length v are the most important parameters for the metasurface structure. These two parameters can affect the electromagnetic properties without increasing the volume of the antenna. Figs. 3(a) and (b) show the simulated results of reflection coefficients and axial ratios (ARs) of the proposed antenna in center frequency with various v and w . The operation frequency decreases as v or w increases. And the AR of the proposed antenna decreases firstly and then increases. Therefore, a minimum AR of 0.34 dB is obtained when $v = 3.7$ mm and $w = 1.2$ mm. Both of them can influence the operation frequency of the proposed antenna in a small frequency range. These influences are accurate, which is convenient for the design.

Figs 3(c) and 3(d) present the simulated reflection coefficients with a series of x and y values respectively. Here, x and y are the position offset in x and y axis direction with respect to the center of the radiation patch. It is obviously that the center frequency keeps invariant when the parameter x or y changes. However, the AR of the antenna changes as the parameters change. It means the center frequency can be kept invariant when the antenna's AR is adjusted. The difference between these two parameters is that x mainly affects the left half resonance peak and y mainly affects the right half resonance peak. They are exactly complementary. When the left half and right half resonance peak are approximately equal to each other, a lowest AR of the antenna can be obtained at the center frequency. In our work, the operation frequency is set at 3.360 GHz. Through adjustments and optimizations, the parameters of the proposed antenna are determined and listed as follows: $a = 22.7$ mm, $b = 24.5$ mm, $d = 0.75$ mm, $v = 3.7$ mm, $r = 1.17$ mm, $w = 1.2$ mm, $x = 0.5$ mm, $y = 1.8$ mm, $\theta = 93^\circ$.

According to the above simulations, a circularly polarized metasurface antenna with low AR is obtained. Fig. 4(a) illustrates the AR curve of the proposed antenna. At the resonance frequency of 3.360 GHz, the AR is nearly zero (0.34 dB). The blue dash line presents 3 dB AR and the 3-dB bandwidth is from 3.350 GHz to 3.368 GHz. In addition, the change trend of the AR agrees well with the results in Figures 3(a) and 3(b). The frequency with lowest AR is corresponding to the center frequency in Figs. 3(c) and 3(d). Fig. 4(b) depicts the simulated and measured reflection coefficients of the proposed antenna.

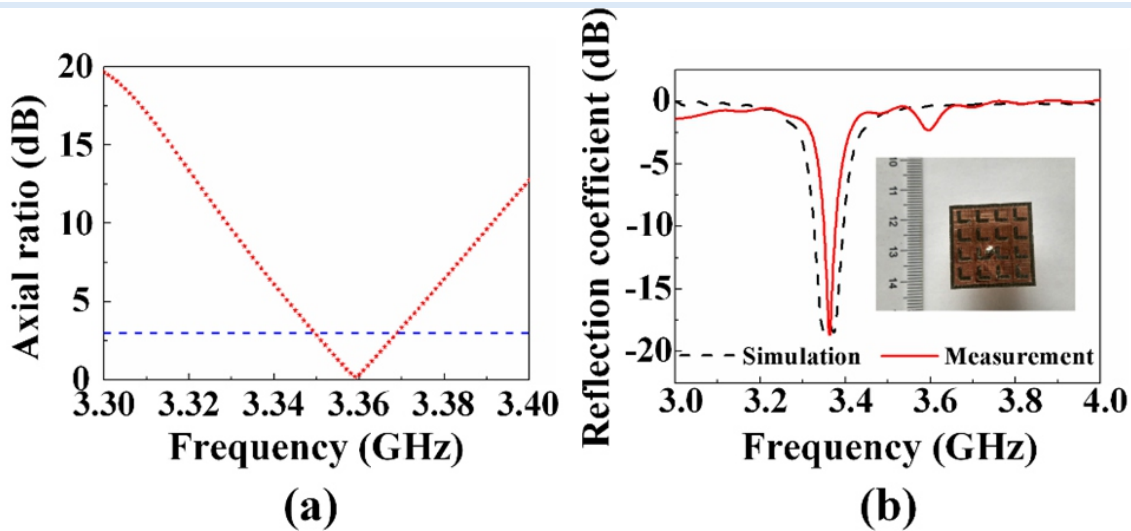


Fig. 4 (a) Simulated AR curve of the proposed antenna. (b) Simulated and measured reflection coefficients of the proposed antenna.

Table 1 Comparison of the Compact Circularly Polarized Antennas.

Structure	3-dB AR Bandwidth (%)	Gain (dB)	Volume
Proposed	0.5	5.3	$0.272\lambda_0 \times 0.272\lambda_0 \times 0.020\lambda_0$
[29]	0.7	3.8	$0.273\lambda_0 \times 0.273\lambda_0 \times 0.013\lambda_0$
[30]	0.5	4.0	$0.288\lambda_0 \times 0.288\lambda_0 \times 0.012\lambda_0$
[31]	0.4	4.6	$0.375\lambda_0 \times 0.375\lambda_0 \times 0.013\lambda_0$
[32]	0.4	3.6	$0.276\lambda_0 \times 0.276\lambda_0 \times 0.014\lambda_0$

It shows that the measured result agrees well with the simulated one. The illustration shows the photography of a fabricated antenna. The overall antenna volume is $0.272\lambda_0 \times 0.272\lambda_0 \times 0.02\lambda_0$, which verifies this proposed antenna is compact. Moreover, the comparisons of size and performance between the proposed antenna and some related published designs are shown in Table 1. The proposed antenna performs well in terms of bandwidth, gain and volume.

3. OAM beams generation based on circularly polarized antenna array discussion

Antenna array that composed of linear polarization antennas is usually used to generate OAM beams. For OAM beam with mode l , the antenna array should be fed with equal magnitude and $2\pi l/N$ phase difference signals, where N is the number of antennas on a circle around the beam axis. In this case, the phase shift device or feed network is essential for the antenna system. To simplify the system, circularly polarized antenna is used in generating OAM beams. The circularly polarized antennas can achieve phase delay by rotating themselves around the antenna center. The basic principle of generating OAM beams with the circularly polarized antenna array is discussed as follows.

According to the mechanism of generating circular polarization, the electrical field radiated by circularly polarized antenna can be written as.

$$\mathbf{E} = \theta A e^{j\phi_1} + \varphi A e^{j\phi_2} \quad (1)$$

Here θ and φ are two orthogonal unit vectors. A is the magnitude of electric field component. ϕ_1 and ϕ_2 denote the phase shift of each field component, satisfying

$$\phi_2 - \phi_1 = \pm \frac{\pi}{2} \quad (2)$$

Thus, the electrical fields of our antenna array can be written as

$$\begin{bmatrix} \mathbf{E}_1 \\ \vdots \\ \mathbf{E}_k \\ \vdots \\ \mathbf{E}_N \end{bmatrix} = \begin{bmatrix} \theta A e^{j\phi_1} + \varphi A e^{j\phi_2} \\ \vdots \\ \theta A e^{j\phi_1 + \frac{2\pi l(k-1)}{N}} + \varphi A e^{j\phi_2 + \frac{2\pi l(k-1)}{N}} \\ \vdots \\ \theta A e^{j\phi_1 + \frac{2\pi l(N-1)}{N}} + \varphi A e^{j\phi_2 + \frac{2\pi l(N-1)}{N}} \end{bmatrix} = \theta A \begin{bmatrix} e^{j\phi_1} \\ \vdots \\ e^{j\phi_1 + \frac{2\pi l(k-1)}{N}} \\ \vdots \\ e^{j\phi_1 + \frac{2\pi l(N-1)}{N}} \end{bmatrix} + \varphi A \begin{bmatrix} e^{j\phi_2} \\ \vdots \\ e^{j\phi_2 + \frac{2\pi l(k-1)}{N}} \\ \vdots \\ e^{j\phi_2 + \frac{2\pi l(N-1)}{N}} \end{bmatrix} \quad (3)$$

The electrical fields of the proposed circularly polarized antenna array can be seen as the superposition of two orthogonal line polarized antenna arrays which can generate OAM beam with mode of l . Therefore, the OAM beams can be generated by circularly polarized antenna array.³³

Fig. 5(a) shows the metasurface circularly polarized antenna array for generating OAM beams at the resonant frequency of 3.360 GHz. In our design, six antennas are evenly distributed on the circumference with radius of $0.5\lambda_0$. To generate the OAM beam with mode of 1, the number of antenna N should be even and satisfies $N > 2|l| + 1$. Hence, N is set as 6. In Fig. 5(a), the red arrows present the directions of the proposed antennas. The angle between the directions of adjacent antennas is 60° , which means 60° phase difference. The simulated radiation pattern of the antenna array and the phase distribution of the generated OAM beam with mode of 1 are depicted in Fig. 5(b) and (c), respectively. The radiation pattern shows center dip due to the phase singularity on the beam axis. The phase distribution is spiral shaped. These characteristics verify the generation of OAM beam with $l = 1$.

To verify the capability of the metasurface antenna array in generating OAM beams, a measurement system was designed, as shown in Fig. 6(a). The antenna array is fed by six-way same signals with the help of vector network analyzer and power divider. Then, the beam generated by the antenna array is measured by a receiving antenna. Here, a proposed circularly polarized metasurface antenna is used as receiving antenna. The operation frequency is set at 3.360 GHz. The one-dimensional amplitude distribution of the OAM beam at propagation distance of $z = 1\text{m}$ is measured and shown in Fig. 6(b). The receive power curve is near symmetric about the center, and the minimum value appears at the center, which implies the doughnut shaped amplitude field is obtained. At the same propagation distance, the measured one-dimensional phase curve is shown in Fig. 6(c). All the measured phase values change in the range from -180° to 180° . There is

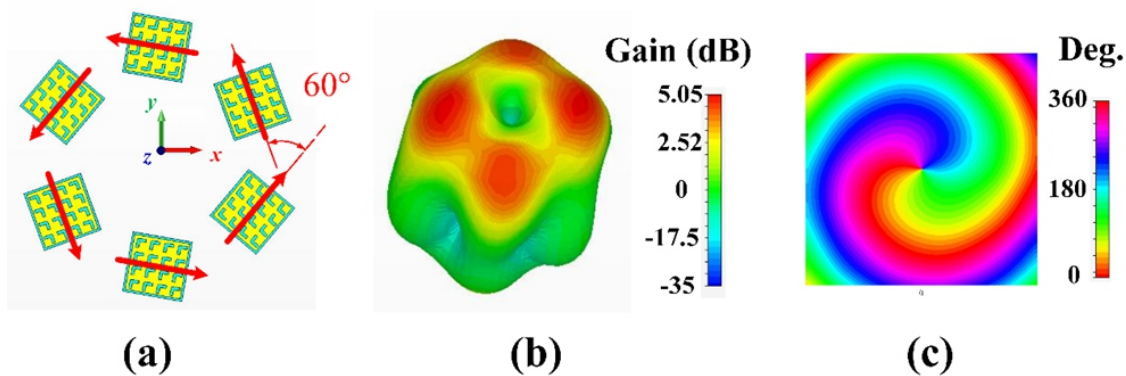


Fig. 5 (a) Configuration of the antenna array. (b) Simulated radiation pattern of the antenna array at the resonant frequency of 3.360 GHz. (c) Simulated phase distribution of the generated OAM beam at the resonant frequency of 3.360 GHz.

a phase singularity at the center of the OAM beams because of the spiral shaped phase distribution. When the receiving antenna goes through the phase singularity, the observed phase value changes dramatically. Therefore, there is an obvious sharp variation at the center of the measured phase curve shown in Fig. 6(c).

To be more intuitive, the near-field amplitude and phase distributions of the OAM beam are measured and illustrated in Figs. 7(a) and 7(b), respectively. The doughnut shaped amplitude field distribution and vortex shaped phase distribution are the remarkable

characteristics of the OAM beams. According to the counterclockwise direction of the vortices, the negative OAM value is determined. Compared with the simulated results shown in Fig. 5, a good match between the simulated fields and the measured ones is easily found. Thus, it is verified that an OAM beam with mode of 1 is generated by the proposed antenna array.

5. Conclusions

A circularly polarized metasurface antenna array has been proposed to

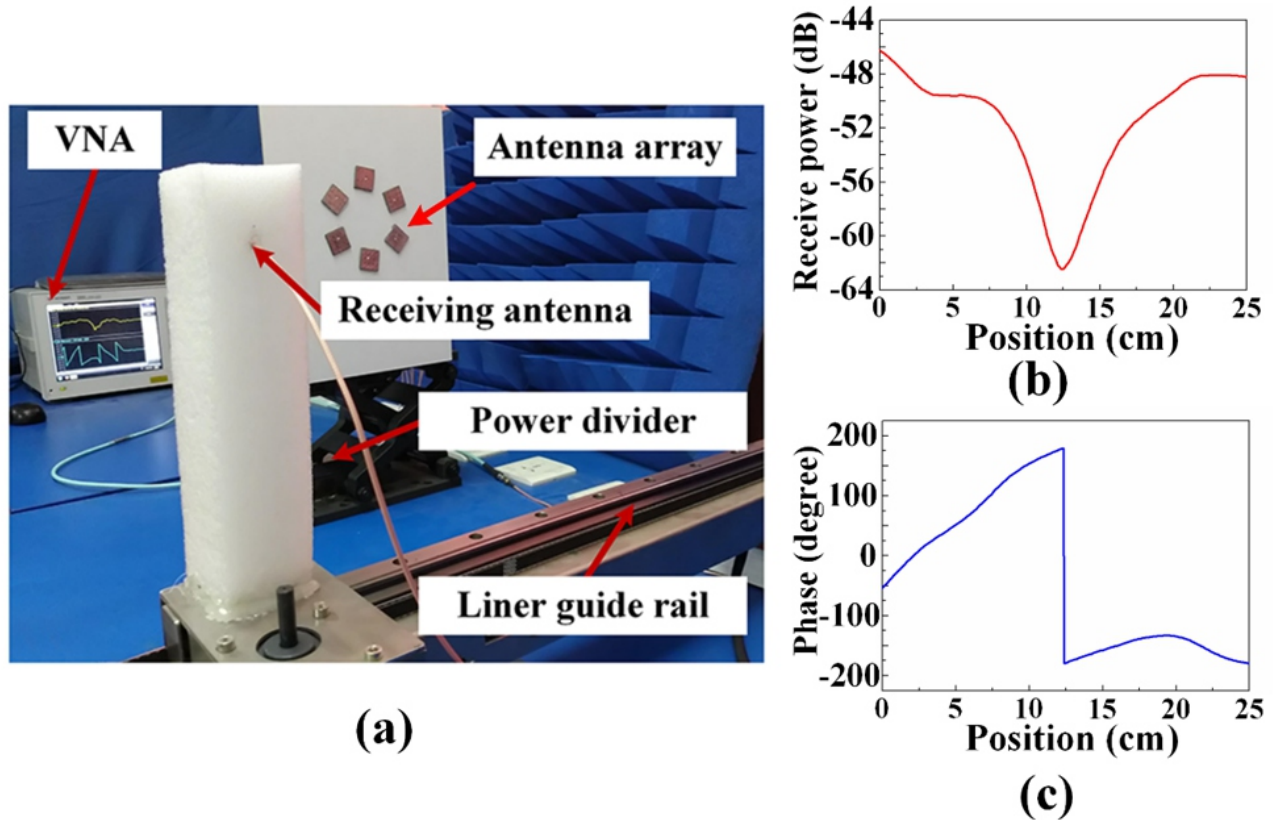


Fig. 6 (a) Measurement system for generating OAM beam. (b) One-dimensional observed receive power and (c) phase distribution of the generated OAM beam at the frequency of 3.360 GHz.

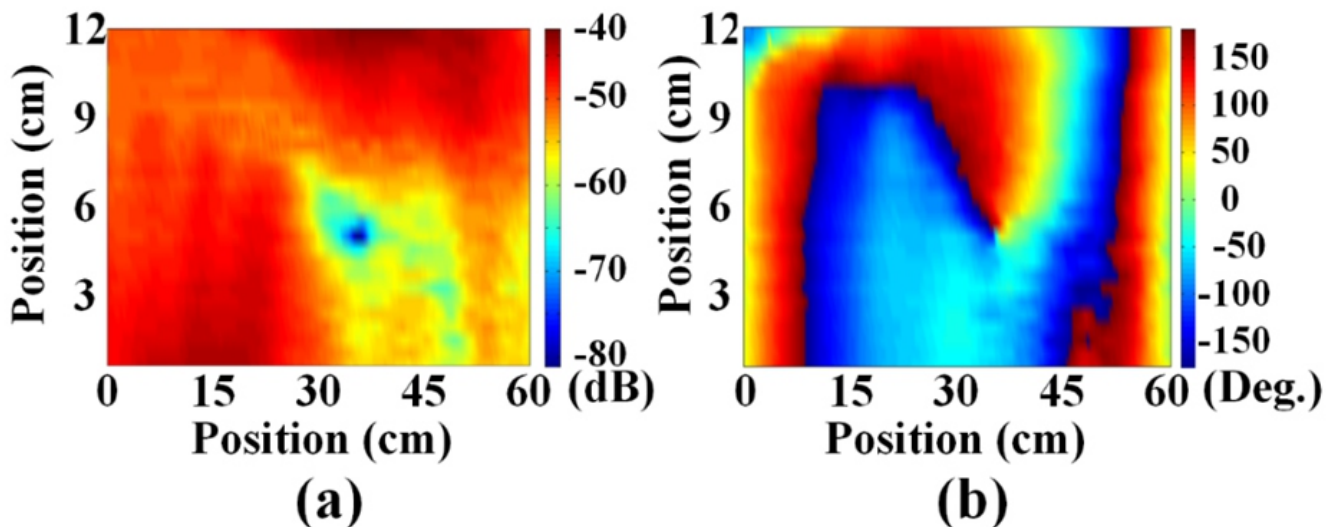


Fig. 7 (a) Measured near-field distribution of amplitude and (b) phase at the frequency of 3.360 GHz.

generate OAM beam. The design process of the circularly polarized antenna becomes more convenient with the help of the metasurface structure. Its resonant frequency is determined by the size parameters and the AR of the antenna can be adjusted by the feed point position. More conveniently, changing the position parameters does not affect the center frequency. The proposed antenna is compact and its gain is higher as compared to other circularly polarized microstrip antennas. An OAM generation and measurement system is designed and the verifying experiments are carried out. The simulated and measured results demonstrate the well performance of the proposed metasurface circularly polarized antenna in generating OAM beams.

Conflict of interest

There are no conflicts to declare.

Acknowledgements

We are grateful to the anonymous reviewers for their valuable comments and suggestions. Financial supports from the National Natural Science Foundation of China under Grant 61774020, Grant 51788104, Grant 51532004, Grant 61671085, Grant 61575028, and Grant 61690195, the Science and Technology Plan of Shenzhen City under Grant 201887776, and the Fund of IPOC BUPT under Grant IPOC2017ZT06 are also gratefully acknowledged.

References

1. Z. N. Chen and X. M. Qing, *IEEE Antenn. Propag. M.*, 2016, **58**, 39-46.
2. Z. Y. Zhang, N. W. Liu, J. Y. Zhao and G. Fu, *IEEE Antenn. Wirel. Pr.*, 2013, **12**, 456-459.
3. K. Bi, X. Y. Wang, Y. N. Hao, M. Lei, G. Y. Dong and J. Zhou, *J. Alloy. Compd.*, 2019, **785**, 1264-1269.
4. J. C. Xu, L. Tao, R. Zhang, Y. N. Hao, S. G. Huang and K. Bi, *Opt. Express*, 2017, **25**, 17099-17104.
5. T. Varum, J. N. Matos, P. Pinho and R. Abreu, *IEEE T. Veh. Technol.*, 2016, **65**, 7219-7227.
6. Y. Yao, X. Cheng, C. Wang, J. Yu and X. Chen, *IEEE J. Sel. Area. Comm.*, 2017, **35**, 1539-1549.
7. T. Nguyen Thi, S. Trinh-Van, K. Y. Lee, Y. Yang and K. C. Hwang, *Electromagnetics*, 2017, **37**, 550-560.
8. Q. Wang, X. Li, L. Y. Wu, P. F. Lu and Z. F. Di, *Phys. Status Solidi R.*, 2018, **13**, 1800461.
9. L. Y. Wu, P. F. Lu, Y. H. Li, Y. Sun, J. Wong and K. S. Yang, *J. Mater. Chem. A*, 2008, **80**, 45-61.
10. P. Schemmel, G. Pisano and B. Maffei, *Opt. Express*, 2014, **22**, 14712-14726.
11. L. Yang, D. Wu and Y. Liu, *Photonics Res.*, 2018, **6**, 517-524.
12. H. J. Xu, K. Bi, Y. N. Hao, J. M. Zhang, J. C. Xu, J. Dai, K. Xu and J. Zhou, *IEEE Antenn. Wirel. Pr.*, 2018, **17**, 2494-2497.
13. K. Nathan and D. R. Smith, *Nat. Mater.*, 2010, **9**, 129-132.
14. J. B. Pendry, D. Schurig and D. R. Smith, *Science*, 2006, **312**, 1780.
15. Z. Deng, Y. Cao, X. P. Li and G. Wang, *Photonics Res.*, 2018, **6**, 443-450.
16. T. Cao, L. Yang, X. Zhang and Y. Zou, *Photonics Res.*, 2017, **5**, 441.
17. X. T. Wang, Y. Cui, T. Li, M. Lei, J. B. Li and Z. M. Wei, *Adv. Opt. Mater.*, 2018, 1801274.
18. A. Mair, A. Vaziri, G. Weihs and A. Zeilinger, *Nature*, 2001, **412**, 313-316.
19. K. Bi, M. H. Bi, Y. N. Hao, W. Luo, Z. M. Cai, X. H. Wang and Y. H. Huang, *Nano Energy*, 2018, **51**, 513-523.
20. M. Dubois, C. Shi, Y. Wang and X. Zhang, *Appl. Phys. Lett.*, 2017, **110**, 190-337.
21. Z. Y. Wei, Y. Cao, X. P. Su, Z. J. Gong, Y. Long and H. Q. Li, *Opt. Express*, 2013, **21**, 10739-10745.
22. I. Staude and J. Schilling, *Nat. Photonics*, 2017, **11**, 274.
23. F. Tamburini, E. Mari, A. Sponselli, B. Thidé, A. Bianchini and F. Romanato, *New J. Phys.*, 2012, **14**, 033001.
24. F. Tamburini, E. Mari, B. Thidé, C. Barbieri and F. Romanato, *Appl. Phys. Lett.*, 2011, **99**, 204102.
25. O. Edfors and A. J. Johansson, *IEEE T. Antenn. Propag.*, 2012, **60**, 1126-1131.
26. J. C. Xu, M. Y. Zhao, R. Zhang, M. Lei, X. L. Gao, S. G. Huang and K. Bi, *IEEE Antenn. Wirel. Pr.*, 2016, **16**, 829-832.
27. M. Padgett and R. Bowman, *Nat. Photonics*, 2011, **5**, 343-348.
28. Y. Nanfang, G. Patrice, M. A. Kats, A. Francesco, T. Jean-Philippe, C. Federico and G. Zeno, *Science*, 2011, **334**, 333-337.
29. Nasimuddin, Z. N. Chen and X. M. Qing, *IEEE T. Antenn. Propag.*, 2012, **60**, 1584-1588.
30. Nasimuddin, X. M. Qing and Z. N. Chen, *IEEE T. Antenn. Propag.*, 2011, **59**, 285-288.
31. D. Wang, H. Wong and C. H. Chan, Small circularly polarized patch antenna. Paper presented at: Antenna Technology (iWAT), 2011 International Workshop on, 2011.
32. X. M. Qing and Z. N. Chen. Compact circularly polarized microstrip antenna for RFID handheld reader applications. Paper presented at: 2009 Asia Pacific Microwave Conference, 2009.
33. X. D. Bai, X. L. Liang, Y. T. Sun, P. C. Hu, Y. Yao, K. Wang, J. P. Geng and R. H. Jin, *Sci. rep.*, 2017, **7**, 40099.

Publisher's Note Engineered Science Publisher remains neutral with regard to jurisdictional claims in published maps and institutional affiliations.